CrossMark

ORIGINAL PAPER

Dielectric properties of three-phase PS-BiFeO₃-GNP nanocomposites

**Srikanta Moharana[1] · Mukesh K. Mishra[1] ·
M. Chopkar[2] · R. N. Mahaling[1]**

Abstract Three-phase nanocomposite films, made up of polystyrene (PS), bismuth ferrite (BiFeO₃; BFO) and conducting particles of graphite nanopowder (GNP), were prepared by solution casting techniques. Using different volume fractions of GNP, the dielectric properties of the nanocomposites were analyzed by impedance analyzer with various ranges of electric fields. To support our discussions, percolation theory was used to know the dielectric behavior of the PS-BFO-GNP nanocomposites and the percolation threshold was observed at 3 vol% of GNP. The dielectric constant of PS-BFO-GNP nanocomposites reached as high as ∼75 at 0.1 kHz, which was much higher than that of pure PS, PS-BFO and PS-GNP nanocomposites. Furthermore, the P–E hysteresis loop study was carried out to observe the ferroelectric behavior of the nanocomposites.

Keywords Polystyrene · Graphite nanopowder · Dielectric constant · P–E loop

Introduction

Currently, the progress of high dielectric constant and high electrical conductivity polymeric nanocomposites have been paying immense interest for their versatile applications in the field of electronic devices, such as gate dielectrics [1–3], microelectronic industry [4], embedded capacitors [5] and other energy storage devices [6]. Several aspects of ceramic filled polymer based nanocomposites have

✉ R. N. Mahaling
rnmahaling@suniv.ac.in; ramnareshmahaling@gmail.com

[1] Laboratory of Polymeric and Materials Chemistry, School of Chemistry, Sambalpur University, Jyoti Vihar, Burla, Odisha 768019, India

[2] Department of Metallurgical Engineering, National Institute of Technology (NIT) Raipur, G. E. Road, Raipur, Chhattisgarh, India

been widely studied in recent few years, among them polymer nanocomposites are most extensively studied because of their ease of processing, better flexibility, high dielectric constant and low loss [7–9]. The more conventional approach of fabricating polymeric nanocomposite materials is to add high dielectric constant ceramic fillers into them. The higher percentage of ceramic filler loading in such polymer based nanocomposites (usually 40 vol%) is the optimum vol% to achieve high dielectric constant of ceramic filled polymer nanocomposites, but more than this volume fraction of ceramic filler loading may bring out a number of drawbacks, such as low mechanical strength, heavy weight and poor process-ability [10–12]. For example, Liyuan Xie et al. [10] reported that the dielectric constant of pristine poly(methyl methacrylate) (PMMA) (3.49) at a frequency of 1000 Hz increases to 14.6 for PMMA/BaTiO$_3$ composite, when in this system the weight percentage of BaTiO$_3$ is as high as 76.88%. In this respect, to overcome these issues, a third component carbon based conductive filler, such as carbon nanotubes (CNTs) [13], carbon fibers [14], carbon black [15] and graphite nanopowders are incorporated into the polymer based ceramic nanocomposite systems. According to the percolation theory, there is an increase in dielectric constant when the conductive fillers are added into the polymer ceramic nanocomposites. Recently, there are various strategies reported on the three-phase nanocomposites, such as sPS/BaTiO$_3$-GNS [16], poly(vinylidene fluoride)(PVDF)/barium titanate (BaTiO$_3$)-CNT [17], PVDF/BaTiO$_3$–carbon fibers [18], PVDF/BaTiO$_3$–Ag [19], PMMA/BaTiO$_3$–Ni [20], Epoxy/BaTiO$_3$–CNT [21], PVDF/BaTiO$_3$–Ni [22]. The attempts of preparing three-phase polymeric nanocomposites filled with conductive fillers, i.e., graphite nanopowder (GNP) and multiferroic ceramic particle, i.e., bismuth ferrite (BiFeO$_3$; BFO) with high electrical conductivity and relatively high dielectric constant has much attracted ever increasing attention in electrical and electronic devices [23]. The BFO has a perovskite structure (ABO$_3$) which is prepared by solid state reaction, sol–gel, co-precipitation and hydrothermal techniques [24]. Usually, these materials have relatively high dielectric constant depending on phase, morphology and particle size. The polymer based multiferroic ceramic nanocomposites are considered to be superior dielectric materials in addition to their various advantages, such as mechanical flexibility, relatively high dielectric constant and low dielectric loss as compared to traditional ceramics [25, 26]. Polystyrene (PS) is an important thermoplastic material having excellent thermal and mechanical properties [27], but it has limited electronic applications due to its low dielectric constant (2.4) and low conductivity. On the other hand, the third component graphite nanopowder (GNP) is an inexpensive polymorphic form of carbon which contains graphene layers stacked into the crystal form and also exhibits interfacial bonding with the polymer matrix so that they possess better dielectric, mechanical and thermal properties [28].

In this communication, we have prepared PS-BFO-GNP nanocomposites containing 10 vol% of BFO with PS and various volume fractions of GNP by solution casting techniques. Among the prepared nanocomposites, 3 vol% of GNP loaded nanocomposite has a high dielectric constant ($\sim$75) and high conductivity at 0.1 kHz. The high dielectric constant and high conductivity nanocomposite materials may be used in suitable electronic devices made from the three-phase nanocomposites. The dielectric and electrical properties of PS-BFO-GNP

nanocomposite films are investigated and also theoretically considered in relation with percolation theory to explain the dielectric behavior of the nanocomposites.

Experimental details

Materials

Bismuth oxide (Bi_2O_3) 99.5% purity and iron oxide (Fe_2O_3) 99% purity were obtained from Merck, India. Polystyrene (PS) polymer was purchased from Alfa Aesar, graphite nanopowder (GNP) (average particle size 50 nm) was obtained from MKNano, USA, and the solvent Toluene (99.0%) was purchased from Loba Chemie Pvt., Ltd., India. All these chemicals were used as received without further purification, and de-ionized water was used throughout the experiment.

Preparation of the BFO particles

The BFO ceramic particles were prepared by the conventional solid state reaction method. First, equi-molar quantities of Bi_2O_3 and Fe_2O_3 were mixed thoroughly in an agate mortar in the presence of air for 2 h and then in methanol for another 2 h. The mixed powders were calcined in a high purity alumina crucible at an optimized temperature of 700 °C for 2 h.

Preparation of PS-BFO-GNP nanocomposites

The fabrications of PS-BFO-GNP nanocomposites were prepared by solution casting techniques. In this process, first the PS was dissolved in toluene and the 10 vol% of BFO was separately ultra-sonicated and added to this solution. After the dissolution of BFO, GNP particles were added to it in desired ratios. Then the prepared solution was vigorously stirred for 30 min to obtain a homogenized solution. The stirring was continued by a mechanical stirrer to ensure that the GNP particles were well dispersed in the polymer matrix. The mixed solution was casted into a polypropylene container and placed in an oven at 65 ± 5 °C for 4 h to obtain nanocomposite films as shown in Scheme 1. For the use of comparison, PS-BFO nanocomposite containing 10 vol% of BFO was prepared by the same procedure in the absence of GNP.

Characterization

The X-ray diffraction spectra of the polystyrene, BFO and their respective nanocomposite films were recorded using an X-ray diffractometer (Mini Flex II, Rigaku, Japan) with Cu K_α ($\lambda = 0.15405$ nm). The microstructural study was analyzed by scanning electron microscopy (ZEISS EVO 18) operated at 30 kV. The dielectric properties of the nanocomposite films were carried out using an impedance analyzer (HIOKI 3532 LCR HiTESTER) at a frequency range
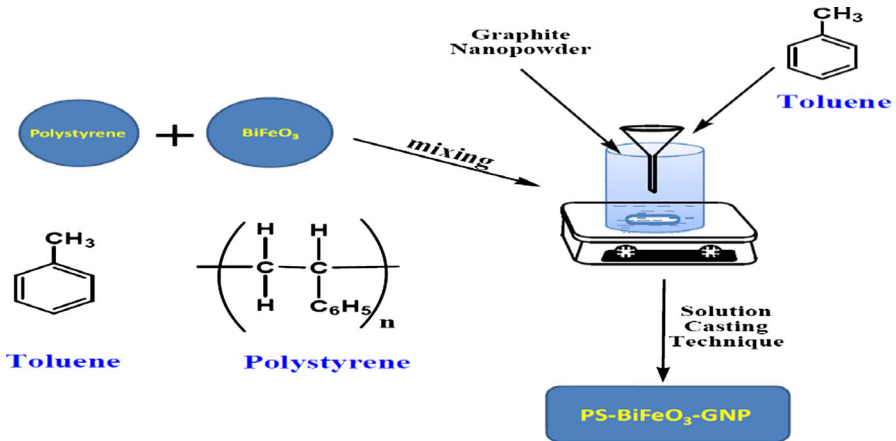
Scheme 1 Schematic representation of PS-BFO-GNP nanocomposite films

(100 Hz–1 MHz) at room temperature. The piezoelectric coefficient d_{33} value was measured with the help of a piezometer (Piezo-test YE2730A).

Result and discussions

X-ray diffraction (XRD analysis)

The structural phase formations of the prepared PS-BFO nanocomposites with various vol% of GNP were investigated using XRD. Figure 1a, b shows XRD patterns of pure BFO and PS-BFO-GNP nanocomposites. As shown in Fig. 1a, among the various diffraction peaks, the presence of (104) and (110) plane at an angle $2\theta \sim 32.1°$ and 32.4° confirms the rhombohedral crystal structure with space groups R3c at room temperature according to JCPDS file no. 71-2494 [29, 30]. From Fig. 1b, it is clearly observed that the incorporation of PS and GNP into the BFO particles may slightly change the structure of BFO and become a distorted rhombohedral in PS-BFO-GNP nanocomposite systems. Similarly, the other peaks located at $2\theta = 26.6°$ and 44.6° may be attributed to (002) and (101) plane of GNP [31].

Microstructural study

Dispersion of particles into the polymer matrix is one of the important factors to enhance the properties of the nanocomposites. The dispersion of fillers in a polymer matrix is not an easy process, as the nanoparticles have a strong tendency to agglomerate. Figure 2a shows an overview of the surface texture of PS-BFO nanocomposite which suggests that the BFO particles are embedded into the polymeric moiety with larger globular form which intends to pull out of the matrix, suggesting lesser reinforcement [32, 33]. However, in case of three-phase PS-BFO-
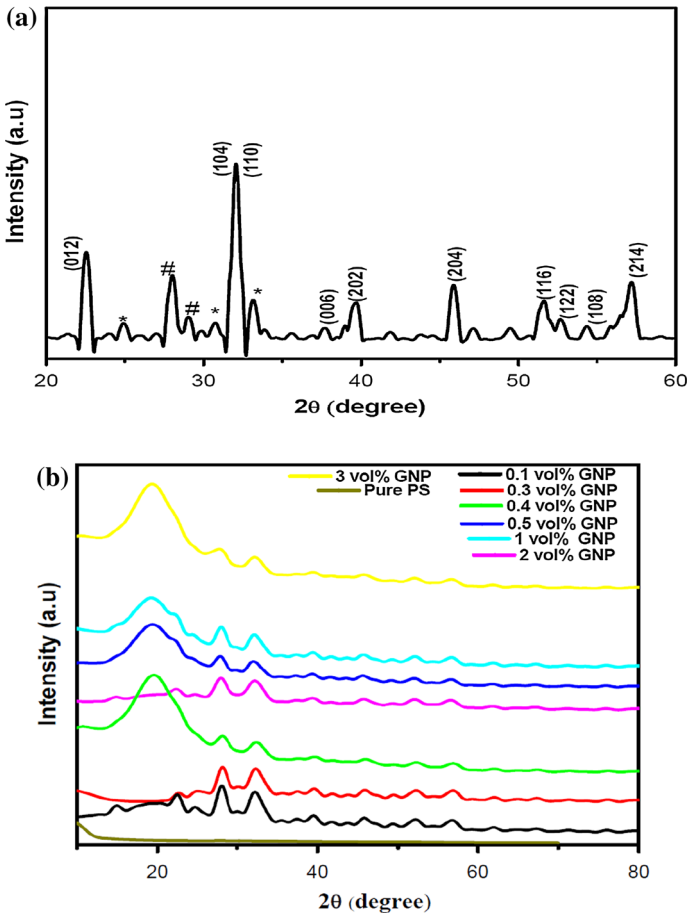
Fig. 1 XRD patterns of **a** pure BiFeO$_3$ and **b** PS, PS-BFO-GNP nanocomposites
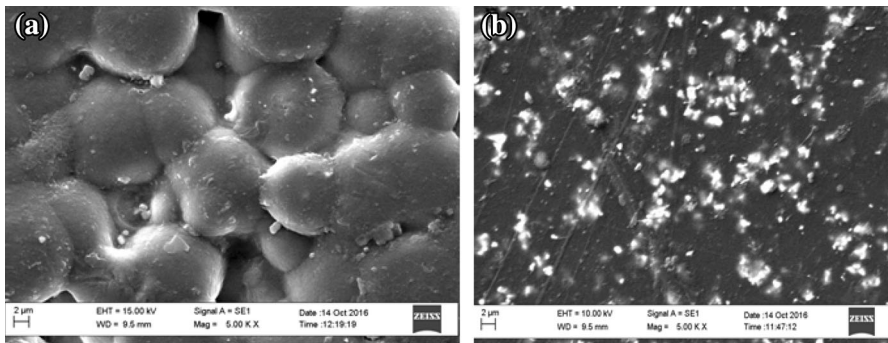

Fig. 2 SEM images of **a** PS-BFO nanocomposites and **b** PS-BFO-GNP nanocomposites with 3 vol% of GNP

GNP nanocomposite systems (as shown in Fig. 2b), the BFO and GNP particles are distributed over the polymeric matrix thoroughly. Simultaneously, the three-phase nanocomposites have more interfacial attachment between the particles and polymer matrix, which may contribute to increase the interfacial polarization and results in enhancement of dielectric constant of the nanocomposites.

Dielectric properties of PS-BFO and PS-GNP nanocomposites

Figure 3a, b shows the dielectric constant and AC conductivity for pure PS, PS-BFO and PS-GNP nanocomposites as a function of frequency at room temperature. It is observed that in case of two phase PS-BFO nanocomposites (Fig. 3a), both the dielectric constant and conductivity is higher than those of pure polystyrene. This behavior may be explained by hopping conduction mechanism of BFO in PS matrix [34]. It shows that at low frequency range the dielectric constant decreases and at high frequency range it maintains linearity as per as PS-BFO nanocomposites is
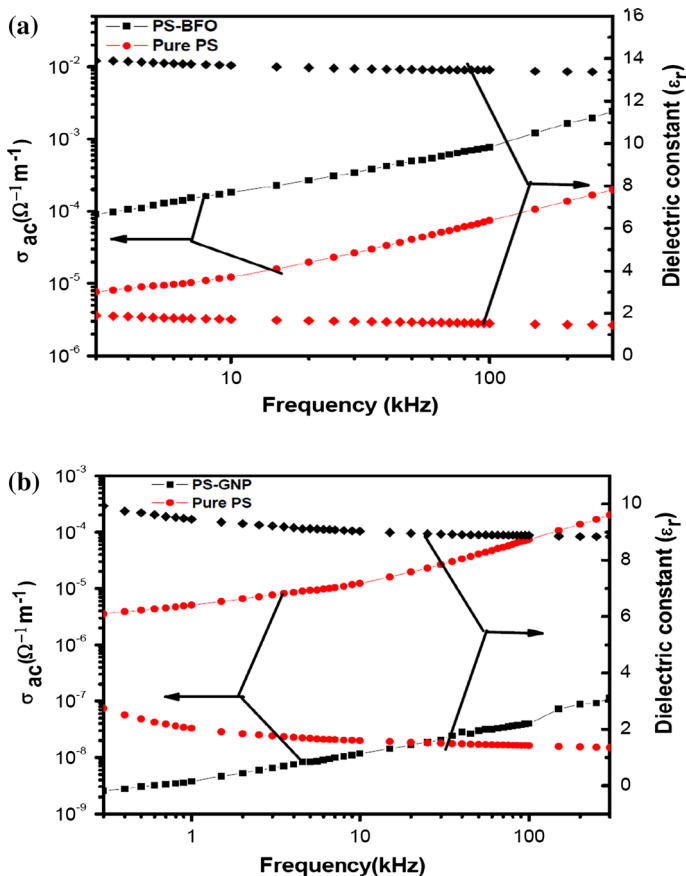

Fig. 3 a, b AC conductivity and dielectric properties of pure PS, PS-BFO and PS-GNP composite containing 10 vol% of BFO as a function of frequency

concerned. From Fig. 3b, it is observed that when the GNP is loaded, the dielectric constant of the PS-GNP nanocomposites shows similar trends to that of PS-BFO nanocomposites, but the conductivity of this nanocomposite is much higher than those of pure PS and PS-BFO nanocomposites. There is an indication of decrease in dielectric constant with increase in frequency and this may be explained by interfacial polarization mechanism [35]. The dielectric constant of PS-BFO and PS-GNP are relatively high, i.e., in the order of fivefold (14) and threefold (9), respectively, in comparison with pure polystyrene whose dielectric constant is ~ 2.4 at 10^3 kHz.

Frequency dependence dielectric properties of PS-BFO-GNP nanocomposites

Figure 4a illustrates the dielectric constant of the prepared nanocomposite films as a function of GNP at 100 Hz. It is observed that the dielectric constant increases rapidly when the GNP content is below 1 vol%, but increases reasonably when GNP content is 3 vol%. The dielectric constant enhances from 32 to ~ 75 which is about 25 times greater than that of pure polystyrene. This enhancement of dielectric constant with respect to 3 vol% of GNP can be explained by percolation theory which is given by the following relation:

$$\varepsilon = \varepsilon_m (fc - f_{GNP})^{-s} \quad \text{for} \quad f < f_c, \tag{1}$$

where ε and ε_m are the dielectric constant of PS-BFO-GNP nanocomposites and in the polymer matrix, f is the volume fraction of conductive fillers and f_c is the percolation threshold concentration of GNP in the polymer matrix, respectively, and s is the corresponding critical exponent related to the materials properties [36]. From Fig. 4 (inset), the best fit of the dielectric constant data to the double log plot of the power law is given by $f_c = 3$ vol% and $s = 0.99$ and it can be explained by Eq. 1. Furthermore, when the GNP concentration increases from 1 to 3 vol%, the dielectric constant slowly increases which is mainly due to the presence of polarization effects in the conductor–insulator interfaces [28]. This increase in dielectric constant may be due to the formation of mini-capacitor network in the PS-BFO-GNP nanocomposite films when the volume fraction of GNP increases. The polarization effect plays a crucial role in the enhancement of dielectric properties of the nanocomposites, especially at low frequency regions [36].

The dielectric loss is an important factor for the improvement of dielectric applications. Figure 4 (bottom left inset) shows the dielectric loss of PS-BFO nanocomposites at various volume percentage of GNP. It is clearly observed that PS-BFO-GNP nanocomposite having 3 vol% of filler loadings has the maximum dielectric loss. This increase in dielectric loss in the three-phase nanocomposites may be due to the isolation effect of BFO particles in the GNP loaded polymer matrix.

Figure 4b shows the frequency dependence of dielectric constant of PS-BFO-GNP nanocomposites for various vol% of GNP. From the figure we can clearly observed that the dielectric constant of the nanocomposite increases with increase in
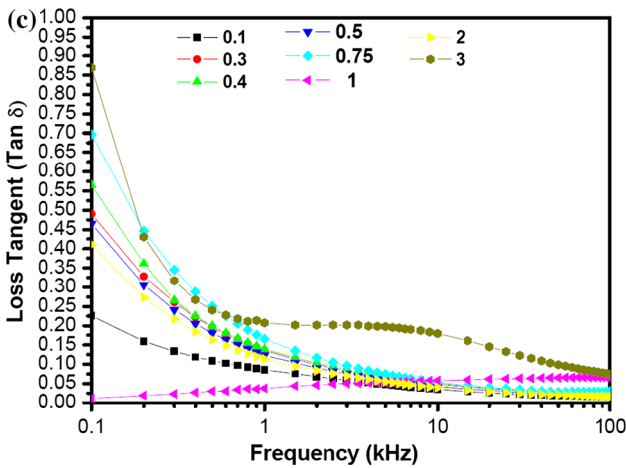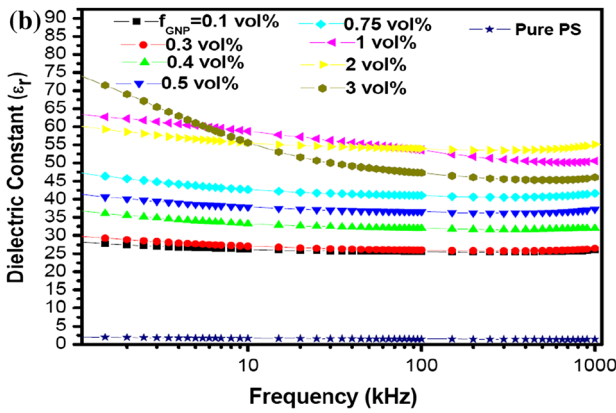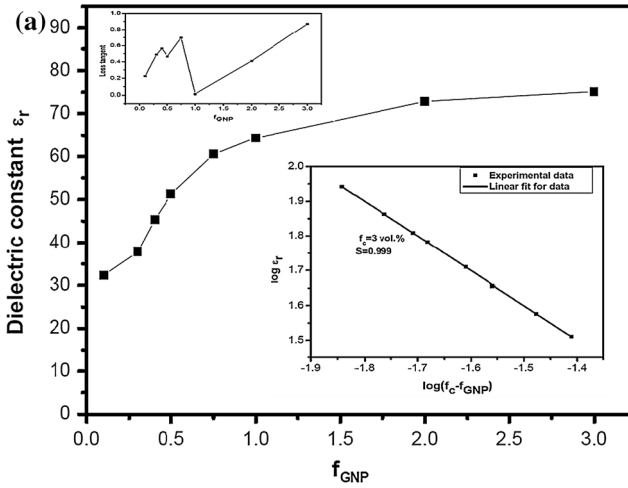
fillers loading but decreases with the increase in frequency. The dielectric constant is always higher at low frequency region and it may be attributed to Maxwell–Wagner–Siller or interfacial polarization effect [22]. The dielectric constant of PS-BFO-GNP nanocomposite at 0.1 kHz (the GNP content is about 3 vol%) is ~75, which is 25, 6 and 8 times higher than those of pure PS, PS-BFO and PS-GNP nanocomposites, respectively. The dielectric loss of PS-BFO-GNP nanocomposites with various vol% of GNP loading as a function of frequency is shown in Fig. 4c. Generally, at low frequency region the dielectric loss of the nanocomposite decreases with an increase in frequency which may be due to the presence of DC or quasi DC conduction on the basis of percolation effect [36].

AC conductivity of the PS-BFO-GNP nanocomposites

Figure 5 shows the variation of AC conductivity of the nanocomposites with various vol% of GNP loading as a function of frequency. It can be clearly revealed that the PS-BFO-GNP nanocomposite with higher volume content of GNP loading possess high conductivity than that of PS-BFO nanocomposite, as clearly shown in Figs. 3a and 5, respectively. However, the AC conductivity of the PS-BFO-GNP nanocomposites increases with an increase in frequency. These types of behaviors are mainly obeyed in good insulating materials [12]. Further, a frequency independent plateau region is obtained at low frequency range. It is usually regarded as dc conductivity (σ_{dC}) and this type of behaviors present in the polymer based nanocomposite filled with conductive fillers. The AC conductivity of the nanocomposites as a function of
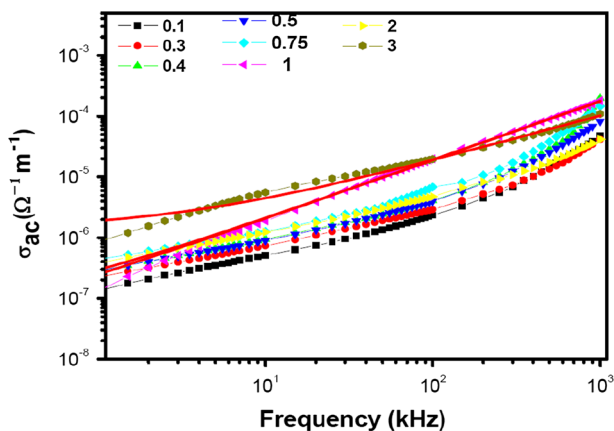

Fig. 5 Frequency dependence AC conductivity of PS-BFO-GNP nanocomposite as a function of frequency at RT

Table 1 AC electrical transport properties of the 1 and 3 vol% of PS-BFO-GNP nanocomposites

PS-BFO-GNP nanocomposite	σ_{dc} (Ω^{-1} m^{-1})	A	n	Goodness of fit (R^2)
1 vol% GNP	2.901×10^{-8}	2.791×10^{-10}	0.966	0.99
3 vol% GNP	1.354×10^{-6}	2.997×10^{-9}	0.754	0.99

frequency can be explained by "ac universal power" law which is given by the following relation [12].

$$\sigma_{ac} = \sigma_{(0)} + Aw^n, \tag{2}$$

where A is the pre-exponential factor and n is the critical exponent ranging from 0 to 1. The value of A, n and σ_{dc} of (1 and 3 vol% of GNP) are calculated by non-linear fitting in Fig. 5 using Eq. 2 and the data are listed in Table 1.

Ferroelectric properties

Figure 6 shows the hysteresis loop of the prepared un-poled PS-BFO-GNP and PS-BFO nanocomposites. Here, we have measured the ferroelectric properties by plotting a graph between electric polarization (P) vs applied electric field (E) which is called P–E loop hysteresis curves. In this figure, we clearly observe that the higher volume content of GNP-loaded three-phase PS-BFO nanocomposites and two-phase PS-BFO nanocomposites are studied. In this work, we choose only 3 vol% of PS-BFO-GNP nanocomposite because it gives best results as compared to that of other volume fraction of GNP. The value of coercive field (2 Ec $\sim$ 1.178 kV/cm) for two-phase PS-BFO nanocomposite is less than that of three-phase nanocomposites whose coercive field value is (2 Ec $\sim$ 1.046 kV/cm). Similarly, in case of two-phase PS-BFO nanocomposites, the value of remnant polarization is (2 Pr $\sim$ 0.162 μC/cm^2) and for three-phase PS-BFO-GNP nanocomposites, the value of remnant
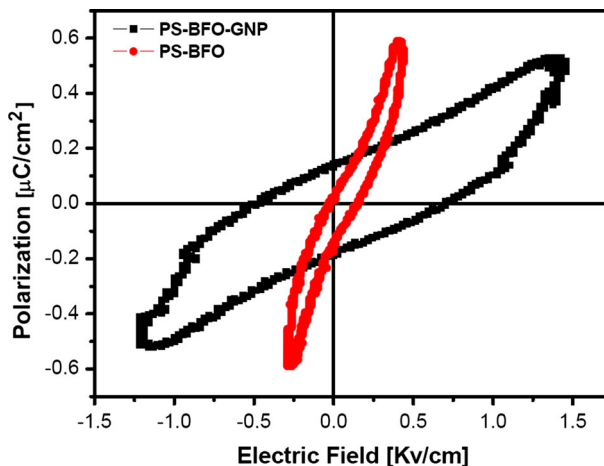

Fig. 6 Hysteresis loop of the PS-BFO-GNP and PS-BFO nanocomposites at room temperature

polarization is (2 Pr $\sim$1.17 μC/cm^2). The remnant polarization is directly proportional to the piezoelectric response of the material [37]. As the remnant polarization of three-phase nanocomposites is higher than that of two-phase nanocomposite system, it shows better piezoelectric properties. Hence, it has more practical applications in electronic industries. Furthermore, the piezoelectric coefficients (d33) are found to be 6 pC/N for three-phase PS-BFO-GNP nanocomposites, and 6.3 pC/N for two-phase PS-BFO nanocomposites. The hysteresis loops and piezoelectric coefficients (d33) confirm that the investigated nanocomposites exhibit ferroelectric properties at room temperature.

Conclusions

In summary, we have prepared the three-phase PS-BFO-GNP nanocomposite films with GNP as conductive filler by solution casting techniques. It is found that the incorporation of GNP into the PS-BFO matrix can effectively enhance the dielectric constant of PS-BFO-GNP nanocomposites. The dielectric constant of PS-BFO-GNP nanocomposites reaches as high as $\approx$75 at 0.1 kHz for percolation threshold at 3 vol% of GNP, which is 25, 6 and 8 times higher than that of pure PS, PS-BFO and PS-GNP nanocomposites. The AC conductivity and ferroelectric properties are improved for three-phase nanocomposites as compared to those of two phases. The enhancement in dielectric and ferroelectric properties supports the possibility of end use utility as new class of polymer-based materials for electronic device applications.

References

1. Popielarz R, Chiang CK, Nozaki R, Obrzut J (2001) Dielectric properties of polymer/ferroelectric ceramic composites from 100 Hz to 10 GHz. Macromolecules 34:5910–5915
2. Wang J, Wu C, Liu R, Li S (2013) P(VDF–TrFE–CFE)-based percolative composites exhibiting significantly enhanced dielectric properties Polym. Bull 70:1327–1335
3. Lei T, Xue Q, Chu L, Han Z, Sun J, Xia F, Zhang Z, Guo Q (2013) Excellent dielectric properties of polymer composites based on core-shell structured carbon/silica nanohybrid. Appl Phys Lett 103:012902–012904
4. Lina M-F, Lee PS (2013) Formation of PVDF-g-HEMA/BaTiO$_3$ nanocomposites via in situ nanoparticle synthesis for high performance capacitor applications. J Mater Chem A 1:14455–14459
5. Luo B, Wang X, Wang Y, Li L (2014) Fabrication, characterization, properties and theoretical analysis of ceramic/PVDF composite flexible films with high dielectric constant and low dielectric loss. J Mater Chem A 2:510–519
6. Nalwa HS (1999) Handbook of low and high dielectric constant materials and their applications. Elsevier Science, Burlington
7. Yuan J-K, Dang Z-M, Yao S-H, Zha J-W, Zhou T, Li S-T, Bai J (2010) Fabrication and dielectric properties of advanced high permittivity polyaniline/poly(vinylidene fluoride) nanohybrid films with high energy storage density. J Mater Chem 20:2441–2447

8. Kim J-Y, Kim H, Kim TY, Yu S, Suk JW, Jeong T, Song Bae MJ, Han I, Jung D, Park SH (2013) A chlorinated barium titanate-filled polymer composite with a high dielectric constant and its application to electroluminescent devices. J Mater Chem C 1:5078–5083

9. Zhang X, Ma Y, Zhao C, Yang W (2014) High dielectric constant and low dielectric loss hybrid nanocomposites fabricated with ferroelectric polymer matrix and $BaTiO_3$ nanofibers modified with perfluoroalkylsilane. Appl Surf Sci 305:531–538

10. Xie L, Huang X, Wu C, Jiang P (2011) Core-shell structured poly(methyl methacrylate)/$BaTiO_3$ nanocomposites prepared by in situ atom transfer radical polymerization: a route to high dielectric constant materials with the inherent low loss of the base polymer. J Mater Chem 21:5897–5906

11. Brandt K, Neusel C, Behr S, Schneider GA (2013) Dielectric behaviour and conductivity of high-filled $BaTiO_3$-PMMA composites and the facile route of emulsion polymerization in synthesizing the same. J Mater Chem C 1:3129–3137

12. He L, Tjong SC (2013) Low percolation threshold of graphene/polymer composites prepared by solvothermal reduction of graphene oxide in the polymer solution. Nanoscale Res Lett 8:132–137

13. Liu H, Shen Y, Song Y, Nan C-W, Lin Y, Yang X (2011) Carbon nanotube array/polymer core/shell structured composites with high dielectric permittivity, low dielectric loss, and large energy density. Adv Mater 23:5104–5108

14. Dang ZM, Fan L-Z, Shen Y, Nan C-W (2003) Study on dielectric behavior of a three-phase CF/(PVDF+$BaTiO_3$) composite. Chem Phys Lett 369:95–100

15. Deniz WDS, Sousa EA, Arlindo EPS, Sakamoto WK, Fuzari GC Jr (2015) Electrical and mechanical characterization of a flexible conducting composite. Polym Bull 72:1787–1797

16. He F-A, Lam K-H, Fan J-T, Chan L-W (2013) Novel syndiotactic polystyrene/$BaTiO_3$-graphite nanosheets three-phase composites with high dielectric permittivity. Polym Test 32:927–931

17. Yao S-H, Dang ZM, Jiang M-J, Bai JB, Nan CW (2008) $BaTiO_3$–carbon nanotube/polyvinylidene fluoride three-phase composites with high dielectric constant and low dielectric loss. Appl Phys Lett 93(18):2905

18. Zhang X, Ma Y, Zhao C, Yang W (2015) High dielectric performance composites with a hybrid $BaTiO_3$/graphene as filler and poly (vinylidene fluoride) as matrix. ECS J Solid State Sci Technol 4:47–54

19. Jiang SL, Yu Y, Zeng YK (2009) Novel Ag–$BaTiO_3$/PVDF three-component nanocomposites with high energy density and the influence of nano-Ag on the dielectric properties. Curr Appl Phys 9:956–959

20. Choi HW, Heo YW, Lee JH, Kim JJ, Lee HY, Park ET, Chung YK (2006) Effects of $BaTiO_3$ on dielectric behavior of $BaTiO_3$–Ni–polymethyl methacrylate composites. Appl Phys Lett 89:132910–132913

21. Park HJ, Hong SM, Lee SS, Kim J, Park M (2006) Effects of CNT/$BaTiO_3$ composite particles prepared by mechanical process on dielectric properties of epoxy hybrid films. IEEE Trans Adv Packag 31(2):417–422

22. Dang Z, Shen Y, Nan CW (2002) Dielectric behavior of three-phase percolative Ni $BaTiO_3$/polyvinylidene fluoride composites. Appl Phys Lett 81(25):4814–4816

23. Wongmaneerung R, Jantaratana P, Yimnirun R, Ananta S (2013) Phase formation and magnetic properties of bismuth ferrite-lead titanate multiferroic composites. J Supercond Nov Magn 26:371–379

24. Fu C, Huo M, Cai W, Deng X (2012) Preparation of bismuth ferrite nanopowders at different calcination temperatures. J Ceram Process Res 13:561–564

25. Mukherjee S, Mitra MK (2014) Characterization of perovskite-spinel nanocomposites (BFO-ZFO) ferrites prepared by chemical route. J Aust Ceram Soc 50:180–187

26. Tamboli MS, Palei PK, Patil SS, Kulkarni MV, Maldarb NN, Kale BB (2014) Polymethyl methacrylate (PMMA)–bismuth ferrite (BFO) nanocomposite: low loss and high dielectric constant materials with perceptible magnetic properties. Dalton Trans 43:13232–13241

27. Tai Q, Kan Y, Chen L, Xing W, Hu Y, Song L (2010) Morphologies and thermal properties of flame-retardant polystyrene/a-zirconium phosphate nanocomposites. React Funct Polym 70:340–345

28. Li YC, Tjong SC, Li RKY (2011) Dielectric properties of binary polyvinylidene fluoride/barium titanate nanocomposites and their nanographite doped hybrids. eXPRESS Polym Lett 5:526–534

29. Moharana S, Mishra MK, Chopkar M, Mahaling RN (2016) Enhanced dielectric properties of surface hydroxylated bismuth ferrite–Poly (vinylidene fluoride-co-hexafluoropropylene) composites for energy storage devices. J Sci Adv Mater Devices. doi:10.1016/j.jsamd.2016.08.008

30. Dutta DP, Mandal BP, Mukadam MD, Yusuf SM, Tyag AK (2014) Improved magnetic and ferro-electric properties of Sc and Ti codoped multiferroic nano BiFeO$_3$prepared via sonochemical synthesis. Dalton Trans 43:7838–7846
31. Li Y, Li RKY, Tjong SC (2009) Fabrication and properties of PVDF/expanded graphite composites. e-Polym 019:1–13
32. Haworth B, Raymond CL, Sutherland I (2001) Polyethylene compounds containing mineral fillers modified by acid coatings. 2: factors influencing mechanical properties. Polym Eng Sci 41:1345–1364
33. Tanniru M, Misra RDK, Berbrand K, Murphy D (2005) The determining role of calcium carbonate on surface deformation during scratching of calcium carbonate-reinforced polyethylene composites. Mater Sci Eng A 404:208–220
34. Prasad K, Prasad A, Chandra KP, Kulkarni AR (2010) Electrical conduction in 0–3 BaTiO$_3$/PVDF composites. Integr Ferroelectr 117:55–67
35. Luo S, Yu S, Fang F, Lai M, Sun R, Wong C-P (2014) Critical interparticle distance for the remarkably enhanced dielectric constant of BaTiO$_3$–Ag hybrids filled polyvinylidene fluoride composites. Appl Phys Lett 104:252903–252904
36. Shang J, Zhang Y, Yua L, Shen B, Lv F, Chu PK (2012) Fabrication and dielectric properties of oriented polyvinylidene fluoride nanocomposites incorporated with graphene nanosheets. Mater Chem Phys 134:867–874
37. Rahman MA, Chung G-S (2013) Synthesis of PVDF-graphene nanocomposites and their properties. J. Alloys Compd. 581:724–730